

**Full System Engineering Design and Operation of an
Oxygen Plant**

James Colvin, Paul Schallhorn, and Kumar Ramohalli
University of Arizona/NASA Space Engineering Research Center

N93-26696

S22-31

158369

P-17

Abstract

This paper describes one area of a project whose general aim is to produce oxygen from the indigenous resources on Mars. After discussing briefly the project's background and the experimental system design, specific experimental results of the electrolytic cell are presented. At the heart of the oxygen production system is a tubular solid zirconia electrolyte cell that will electrochemically separate oxygen from a high-temperature stream of Coleman grade carbon dioxide. Experimental results are discussed and certain system efficiencies are defined. The parameters varied include 1) the cell operating temperature; 2) the carbon dioxide flow rate; and 3) the voltage applied across the cell. The results confirm our theoretical expectations.



Introduction

Background

A primary concern for any mission to Mars must be how much energy will be necessary to complete the mission. An important consideration has to be: Should we continue to bring all propellants with us from Earth, or should we take advantage of the many known resources that are available to us on Mars? With this idea in mind and wishing to expand on the success of the Martian Viking program, Ash, Dowler, and Vars¹ in the late seventies envisioned an in-situ propellant plant which would make use of the Martian atmosphere to produce an oxygen and methane propellant.

The heart of this system would be an array of yttria stabilized zirconia solid electrolyte cells. These cells have the ability to selectively conduct oxygen ions, thus allowing the production of pure oxygen. The oxygen plant has undergone many changes since it was first envisioned by Ash¹ et al. Frisbee and Lawton have done extensive work on improving the overall system by reducing the total system mass and increasing the total system reliability.²⁻⁴

Their improved system would have the Martian atmosphere drawn in through an electrostatic dust filter, which is necessary as there are numerous long-term dust storms on the Martian surface. The atmosphere, which consists of approximately 95% carbon dioxide, will be drawn into the system by a CO₂ adsorption compressor. Present plans³ require the atmosphere to be compressed from the ambient pressure of 6.8 mb to a pressure of 1 bar for delivery to the cathode of the electrolyte. Before entering the zirconia array, the flow will pass through a heat exchanger which will raise the temperature from the CO₂ compressor's exit temperature of 600 K to approximately 1000 K. The source of the heat for the heat exchanger is the exhaust flow from the array. Once the flow has entered the array, it will be further heated to a temperature of 1273 K.

This temperature is sufficient to partially dissociate the carbon dioxide into carbon monoxide and diatomic oxygen. The O₂ will be increased to 4 bar. The cell's exhaust will consist of mostly CO₂ with some CO resulting from the removal of O₂. The O₂ produced at the anode will pass through a radiator where it will be cooled from 1270 to 250 K with a pressure of 3.8 bar. The O₂ will next pass through an O₂ adsorption compressor where its pressure will be increased to 28 bar and its temperature to 400 K. After passing through a radiator, the flow will be cooled to 230 K. The O₂ will be finally cooled to 100 K by a molecular adsorption cryo-cooler refrigerator and stored for its final use. The use could initially be the oxidizer for the propellant necessary to return a Martian sample

to earth, and then eventually, life support for a manned Martian mission.

Yttria-Stabilized Zirconia Solid Electrolyte

In Lawton's work,³ he lists development risk factors for components. In his option III, the oxygen cell is the only component still listed as risk factor 4, meaning "there are still serious problems that must be addressed as well as some intensive development required." This is an area of current research. Further details were worked out in Reference 5. Since the Martian atmosphere is predominantly CO₂, the remainder of this report will refer to the atmosphere as CO₂. The CO₂, when it enters the cell array, will be heated to 1273 K. At this temperature, the CO₂ will begin to partially dissociate into CO and O₂. The zirconia electrolyte is sandwiched between two porous platinum electrodes. The dissociation will occur at the cathode with the O₂ entering the electrode and moving towards the electrode-electrolyte interface. The driving force for this movement is the partial pressure gradient developed by the electrolyte removing oxygen from the interface area. Once the O₂ reaches the interface, it is further reduced to monatomic oxygen. The oxygen received two electrons from the negative electrode and becomes an oxygen ion and begins to migrate through the zirconia electrolyte towards the anode. Upon reaching the anode, the ion will release its two electrons to the positive electrode and then recombine with another oxygen atom to reform the O₂ molecule. Qualitatively, this describes the oxygen separation process. *Figure 1⁴* shows this process schematically.

Richter performed the initial intensive testing of this electrochemical process with the aim of quantifying this physical procedure.⁶ His work was performed using a tubular zirconia cell. He developed the basic thermodynamic and electrochemical models for the reduction of CO₂ and the subsequent production of O₂. A few years later, Sutor continued the investigation.⁷ In his experiment, he used the disk geometry for his cells. Additionally, he investigated the use of different electrode materials. Although his supply gas was air, many of his results can also be applied when CO₂ is the supply gas.

In this study, zirconia cells with the tubular geometry were used. The aim was to develop various cell efficiencies by varying several system control parameters. These parameters were: the potential applied across the electrolyte, the electrolyte operating temperature, and the incoming CO₂ flow rate. We would like to know how the CO₂ production rate varies as a function of these parameters. The various efficiencies include the cell's Nernst efficiency (a measure of the theoretical energy required against the actual energy put into the system). The definitions of these efficiencies will be

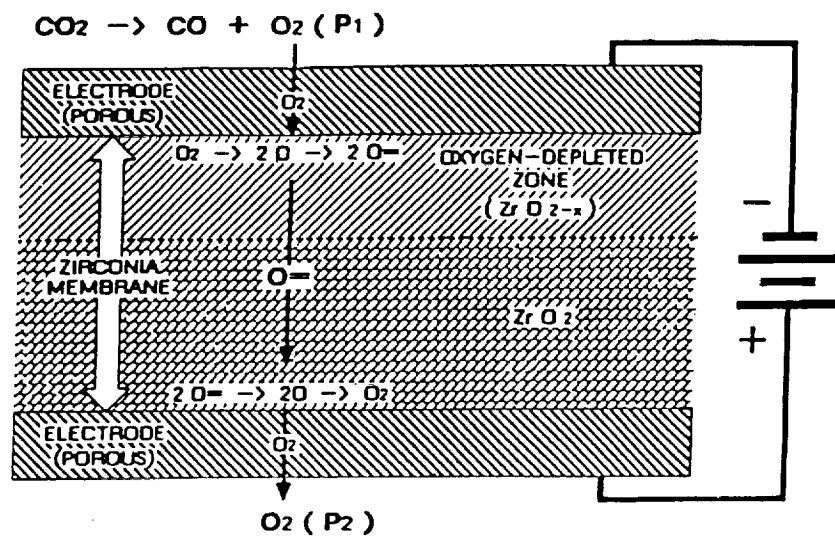
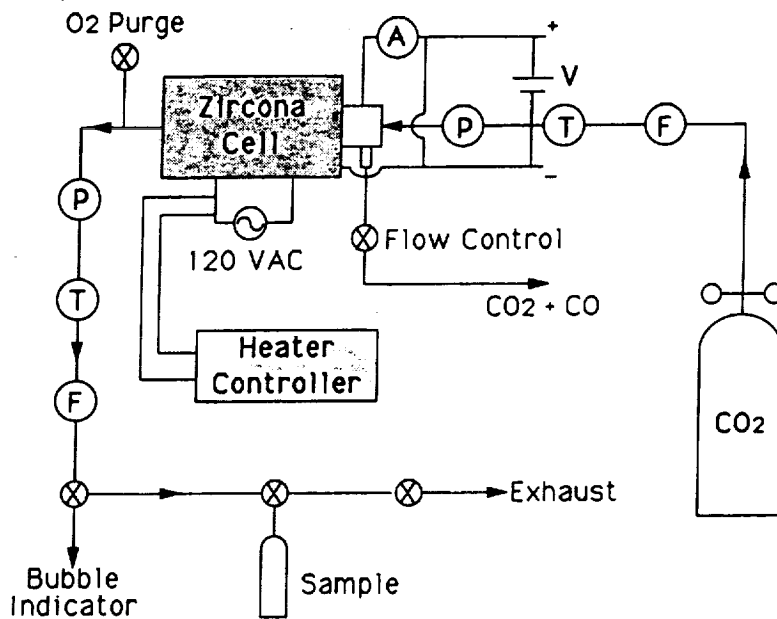


Fig. 1 Oxygen migration through the ZrO_2 cell.



- (T) Thermocouple (P) Pressure Transducer
 (F) (V) (A) Flow/Volt/Current Meter

Fig. 2 Single cell test bed (schematic).

developed later in this report. The single zirconia cell test bed currently being studied is shown schematically in *Figure 2*. The test bed consists of the following: 1) one tubular zirconia cell; 2) one voltage DC power supply; 3) two digital multimeters; 4) two ceramic clam shell heaters; 5) one Watlow heater controller; 6) Kaowool type ceramic insulation; 7) one O₂ pressure transducer (0-500 psia); 8) one CO₂ pressure transducer (0-500 psia); 9) one O₂ flow meter (0-50 sccm); 10) one CO₂ flow meter (0-5000 sccm); 11) three ktype thermocouples; (12) Coleman grade CO₂ for supply gas; 13) one PC/386 processor for data acquisition; and 14) Varian model 3700 gas chromatograph.

To simulate the Martian atmosphere, which contains approximately 95% CO₂ and only 0.13% O₂, Coleman grade CO₂ was used to supply the test bed. This grade contains less than 20 ppm O₂. The flow was maintained at slightly above local atmospheric pressure (13.7 psia) at a temperature of 75°F. The flow rates were varied between 38 and 1475 sccm. Flow would enter the zirconia tube through a 1/8 in. alumina tube and then pass to the far end of the zirconia chamber (see *Figure 3*). The clam shell heaters are centered about the middle 7 in. of the zirconia device. This means heating of the flow will begin in the alumina tube. Exiting the alumina tube, the flow reverses direction while continuing to be heated and flows across the cathode of the electrolyte. The CO₂, now heated, begins dissociation and is drawn to the cathode. The free stream is now a mixture of CO₂, CO, and O₂. O₂ is dissociated to monatomic oxygen at the electrode-electrolyte interface and electrochemically conducted through the zirconia to the anode while the CO₂ and CO exhaust pass out through the exit of the tube. The supply CO₂ flow rate is controlled by a metering valve in the exhaust flow. The O₂ produced (at approximately 13.7 psia) flows through the mass flow meter and then can be directed to a water bubbling device, a sample cylinder, or directed to the gas chromatograph for analyzing. The zirconia electrolyte and its platinum electrode have an upper temperature limit of 1150°C where a phase change in the zirconia will take place. A critical voltage limit of 2.23 VDC was assumed in accordance with the work of Frisbee.⁴ Keeping below this potential will prevent the oxygen from being driven from the zirconia lattice structure causing permanent damage to the cell. With these material limits in mind, a self-imposed limit of 1100°C, and 2.0 VDC was used during all testing.

Single-Cell Test Results

Fundamental Results

A series of tests were conducted to attempt to characterize the effects of temperature, cell potential, and carbon dioxide flow rate on the production rate of oxygen. During testing, the temperature was varied from 800 to 1100°C in increments of 25°. Cell potential varied from approximately 0.6 to 2.0 VDC in increments of 0.1 volts. The CO₂ flow rate varied from 38 to 1475

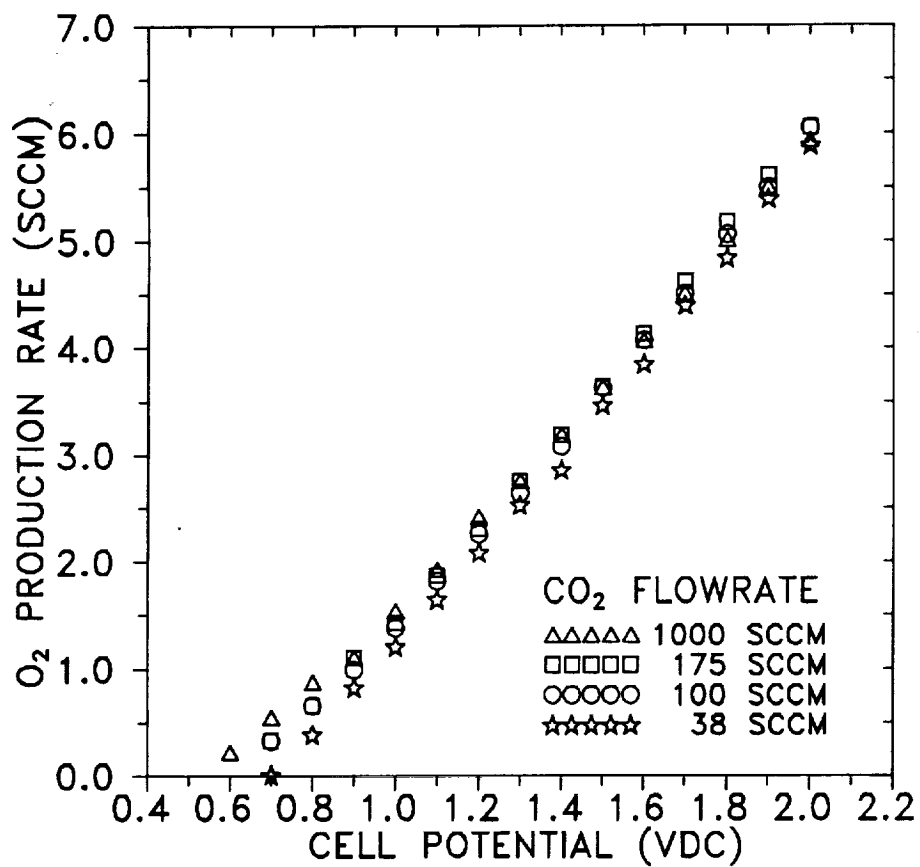


FIGURE 4

SINGLE ZIRCONIA CELL SCHEMATIC

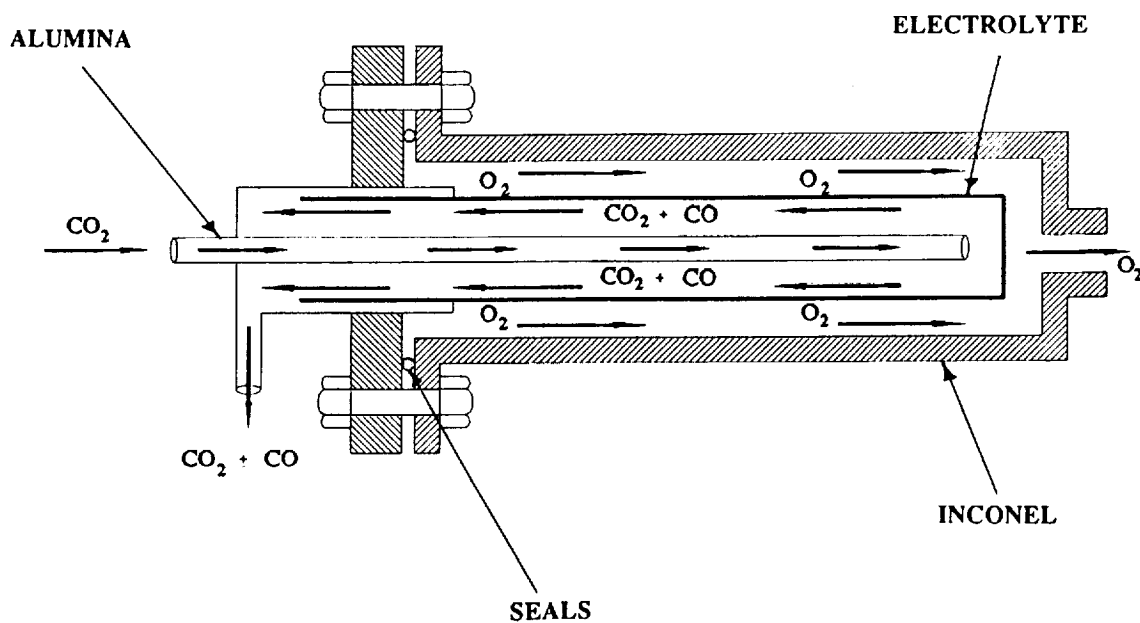


FIGURE 3

sccm. The following figures show the results of this testing. *Figure 4* shows the dependence of the production rate of O₂ on the applied cell potential for a variety of CO₂ flow rates at a temperature of 1000°C, while *Figure 5* displays the production at four different temperatures at a CO₂ flow rate of 138 sccm. Note, on both Figs. 4 and 5, the second-order dependence of oxygen production on the applied cell potential.

Figure 6 demonstrates the dependence the oxygen production has on the temperature of the cell with an applied cell potential of 2.0 VDC. Notice the weak dependence the oxygen production has on the carbon dioxide flow rate. *Figure 7* presents the oxygen production vs cell temperature at a carbon dioxide flow rate of 138 sccm. *Figure 7* also clearly depicts the dependence on voltage of the oxygen production rate.

Figure 8 indicates the O₂ production rate dependence on the CO₂ supply flow rate for an applied cell potential of 2.0 VDC. This is the most graphic illustration of the lack of dependence on the carbon dioxide flow rate for the oxygen production rate, especially for CO₂ flow rates greater than about 200 sccm. *Figure 8*, like the previous figures, shows the dependence on the temperature for the O₂ production rate.

Interpretation of the Results

The results of the extensive system analysis can be discussed in five areas: 1) flow rate effects, 2) mass flow ratio, 3) oxygen conversion efficiency, 4) Nernst efficiency, and 5) the system efficiency. Each of these areas will be addressed in order.

The flow rate effects were the easiest to interpret. The basic schematic is shown in *Figure 2*. It was initially found that the oxygen yield rate (production rate) increased as the CO₂ flow rate increased, but only up to a certain point, after which increased flow rate actually resulted in the decrease of the yield of oxygen. This was observed while other parameters such as cell voltage and cell temperature were held constant. It was suspected that the carbon dioxide may not have had sufficient residence time within the heated cell to achieve the required temperature at the high flow rates. To verify this hypothesis, a simple thermal diffusivity analysis was performed, after confirming that the flow within the tube is indeed laminar via simple Reynolds number calculation. The residence time is given by l/u , where l is the tube length and u is the mass averaged velocity. The characteristic time for heat transfer within the tube is given by $(d/2)^2/\alpha$, where d is the cell inside diameter and α is the thermal diffusivity ($k/\rho c_p$) of the carbon dioxide at high temperatures. As can

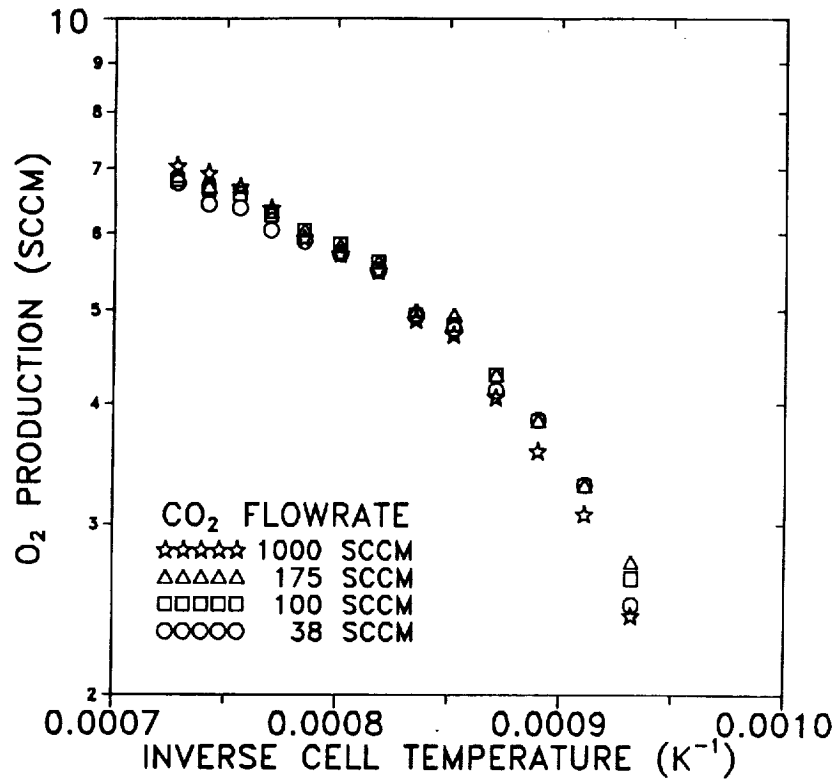


FIGURE 6

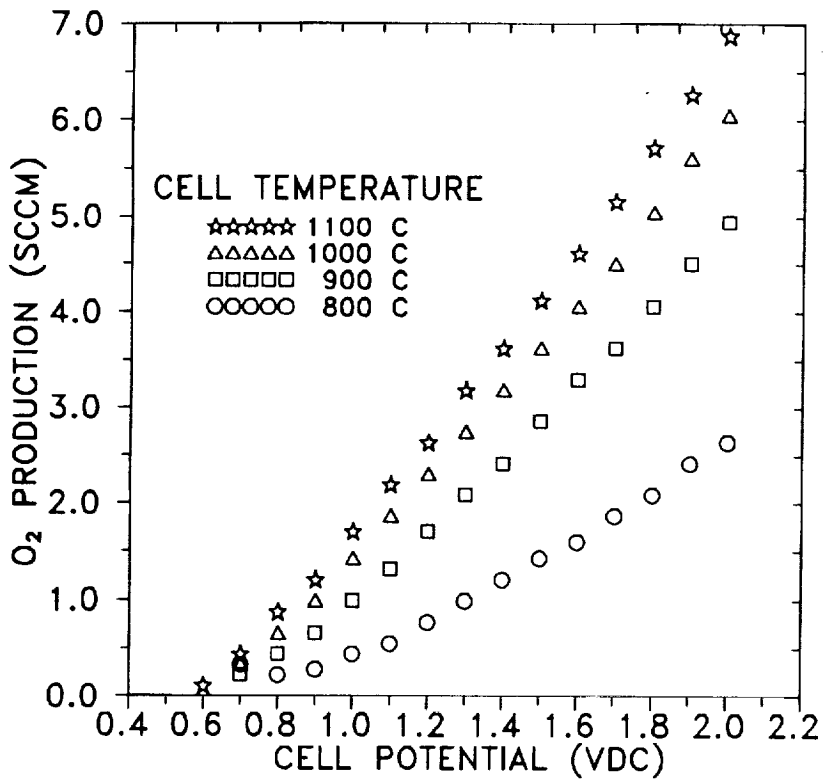


FIGURE 5

be seen in *Figure 9*, the peak occurs almost precisely where the two times become equal. It is thus clear that up to the point where the residence time is sufficient to bring the carbon dioxide to the requisite temperature, the production rate of the oxygen increases with the flow rate, but beyond this point the production rate falls off. It would be instructive to measure the actual gas temperature, and not merely the cell wall temperature as is done in the experiments reported here.

The mass flow ratio (the mass production rate of O₂ divided by the CO₂ supply mass flow rate) is of much interest. This is due to sizing constraints within scaled-up systems such as the primary carbon dioxide compressor, the heat exchanger, and the radiators. For these reasons, Figs. 10 and 11 plot the mass flow ratio vs CO₂ flow rate and temperature, respectively.

In previous studies of the propellant production plant, the emphasis was placed on sizing of the total production system.²⁻⁴ For these studies, oxygen conversion efficiencies of 25-30% were used when considering the estimated surface area needed to produce a required amount of oxygen per day. The use of these efficiencies was necessary to minimize oxygen plant mass. However, when considering the operation of the zirconia cell alone, *Figure 12* shows the complete range of oxygen conversion efficiencies.

As the concern of this report is the complete characterization of the zirconia electrolytic cell, all conversion efficiencies must be investigated. Richter, in his early work⁵ on the reduction of CO₂ began with the basic Nernst relation:

$$E_N = \frac{RT}{zF} \ln \left[\frac{P_2}{X_{O_2} P_1} \right]$$

Here, E_N is the Nernst voltage, T is the temperature (K), z is charge/mole ($z = 4$), R is the universal gas constant, and F is the Faraday constant. Additionally, P_2 is the pressure at the anode while X_{O_2} P_1 is the partial pressure of the oxygen in the supply CO₂ flow stream at the cathode. Richter then continued with his model and developed an instantaneous Nernst potential

$$E_{Ni} = \frac{RT}{zF} \ln \left[\frac{P_2}{\left(\frac{K(1-n)}{n} \right)^2} \right]$$

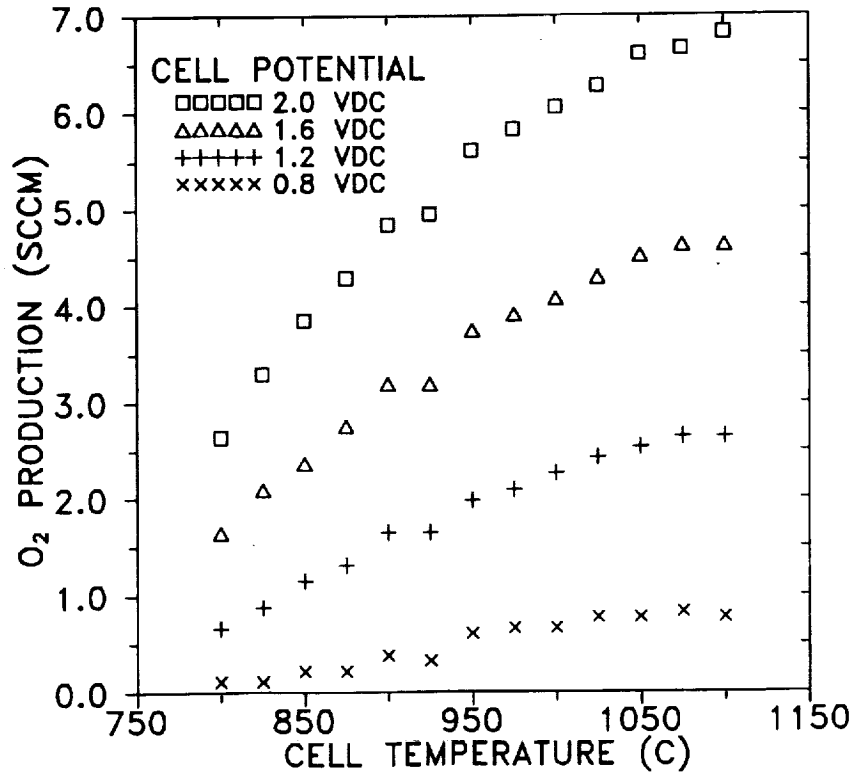


FIGURE 7

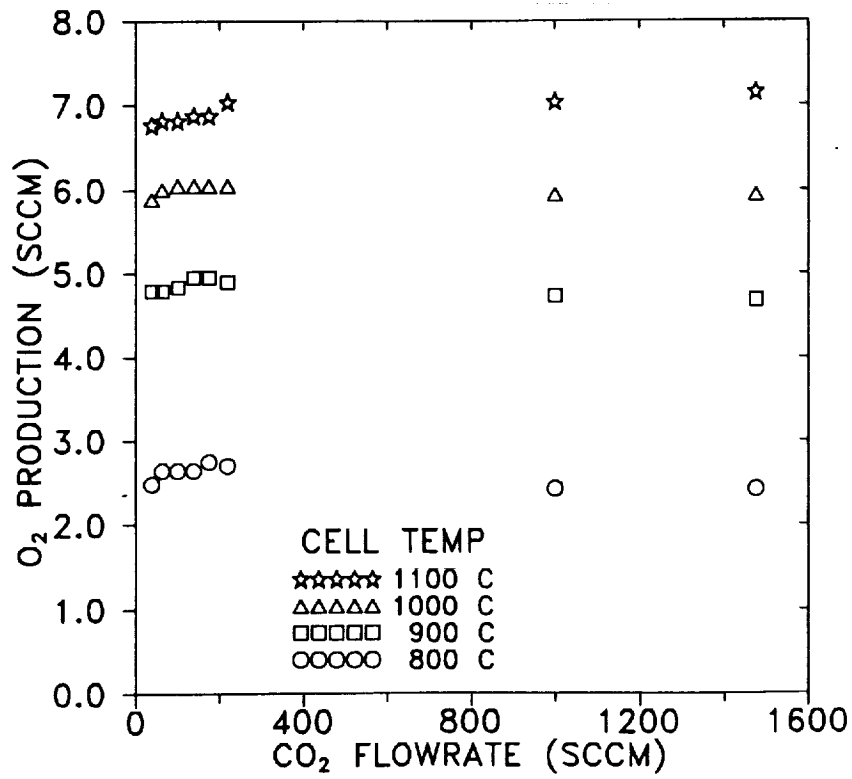
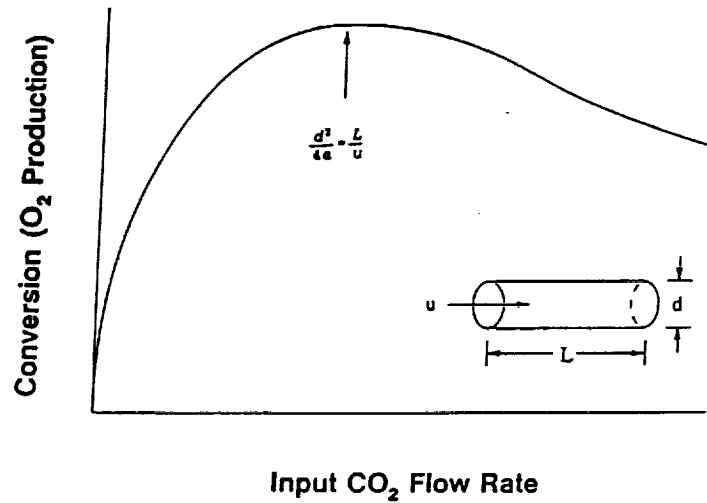


FIGURE 8

EXPLANATION OF FLOW-RATE EFFECT



[α is the thermal diffusivity of CO₂ at 1000° C]

Fig. 9 Thermal diffusivity vs residence time.

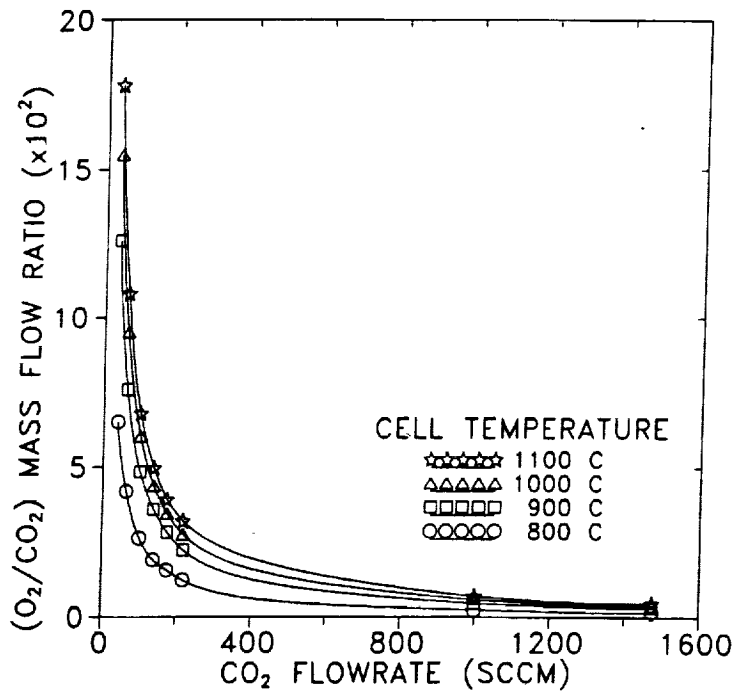


Fig. 10 O₂/CO₂ mass flow ratio vs CO₂ flow rate, cell potential = 2.0 VDC.

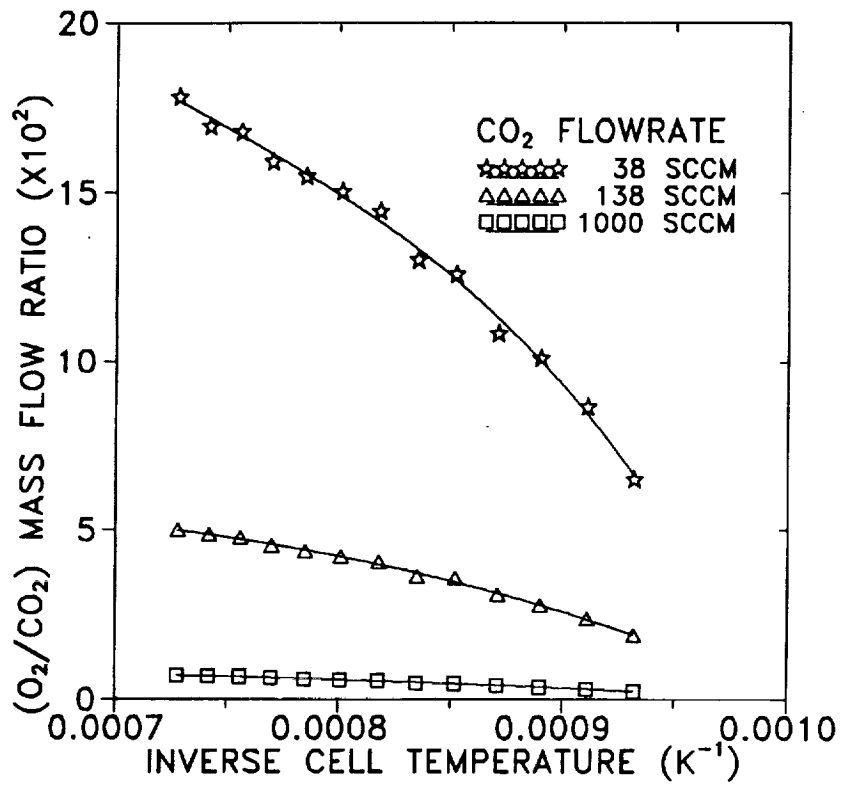


FIGURE 11

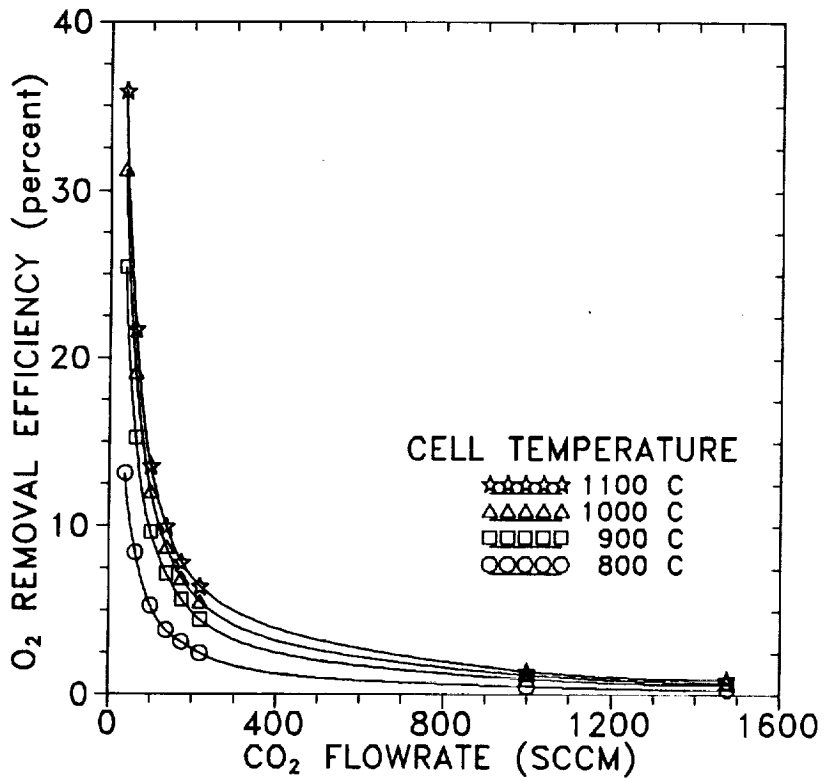


FIGURE 12

In this equation, K is the normal equilibrium constant and n is the mole fraction of CO_2 reduced to CO . The value n can be calculated from this equation:

$$n = C \left(\frac{I}{\dot{V}_{\text{CO}_2}} \right)$$

The value C is a constant from Richter's work ($C = 6.969$), I is the measured current produced across the cell, and \dot{V}_{CO_2} is the volumetric flow rate of the supply CO_2 stream. The current (A) was measured experimentally, as well as the volumetric flow rate of the CO_2 (sccm). The cell temperature (K) was measured by a k -type thermocouple positioned at the outside wall of the cell, and the pressure of the O_2 collection side of the cell was assumed to be one atmosphere. Using the proper values for the equilibrium constant K ,⁸ there was enough information available to calculate the instantaneous Nernst voltage. Richter cautions the use of this equation by stating that it is valid only if the critical voltage over the cell is not reached. The critical voltage can be defined as the potential which will be just sufficient to begin removing oxygen from the lattice of the zirconia. This process would be apparent from an "elbow" being observed in the current vs potential plot in the higher potential range (> 2 VDC). *Figure 4* shows this potential has not been reached due to the lack of an elbow. According to Richter then, the potential can be expressed as a function of the operating temperature and the actual amount of O_2 removed and not the partial pressure of the O_2 at the cathode. The instantaneous Nernst potential was used in defining the Nernst efficiency:

$$\eta_N = \frac{E_{Ni}}{E_{act}}$$

This equation shows the Nernst efficiency is the ratio of the theoretical potential divided by the actual potential (E_{act}). What this indicates is the instantaneous amount of cell overpotential. *Figure 13* shows the results of this analysis.

It is apparent from this figure that the amount of cell overpotential rises as the applied cell potential rises. One source of this overpotential could be the pressure drop through the porous electrode. It is important to remember that from *Figure 4*, the rise in O_2 production is almost directly proportional to the potential applied to the cell. Ash⁹ et al. point out that experiments have shown that as the O_2 production rate rises, there is an increase in the pressure drop across the negative

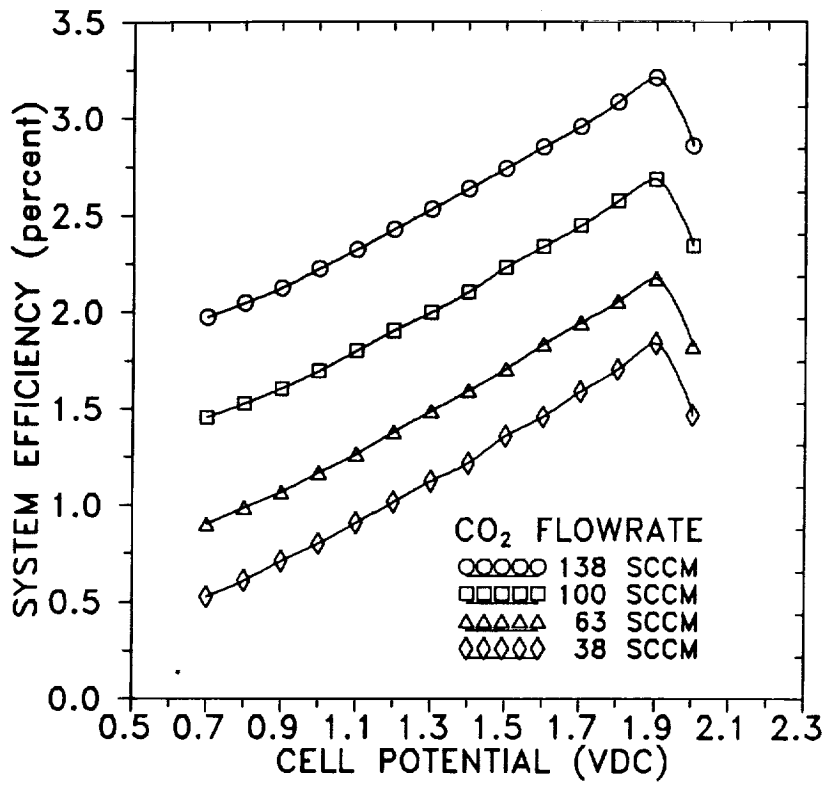


FIGURE 14

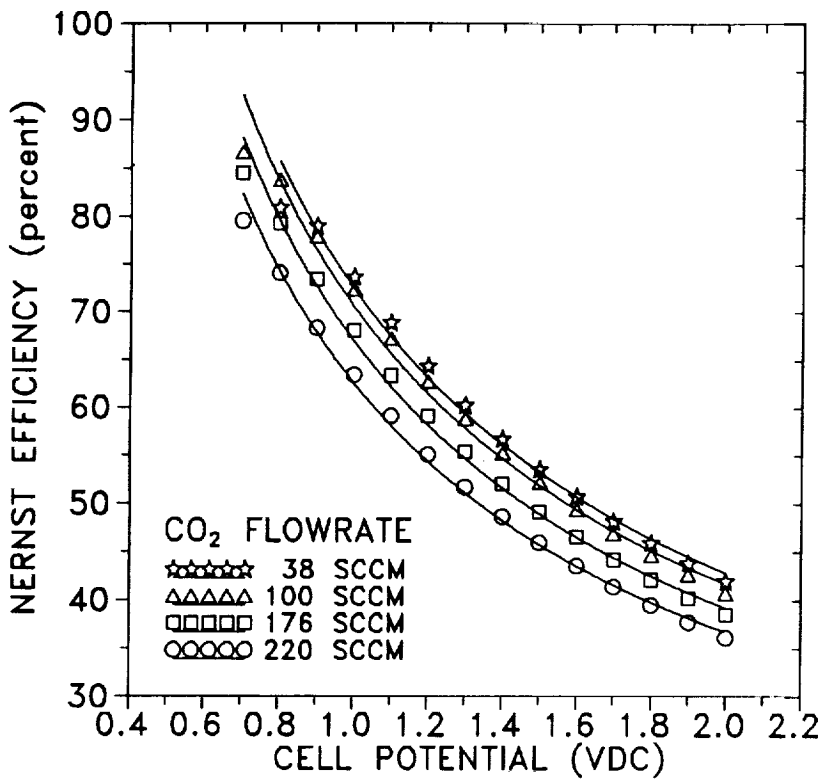


FIGURE 13

electrode which can approach the partial pressure of the oxygen in the CO₂ stream resulting in an ever increasing pumping power requirement. Another possible source of the overpotential is slow diffusion, adsorption, or dissociation processes near the electrode-electrolyte interface of the cell resulting in concentration overpotential.¹⁰ This report also states the possibility of a transition overpotential due to slow electrochemical reaction. The sources of overpotential cannot be experimentally determined with this system as currently constructed, but any future characterization of the zirconia electrolyte should definitely seek to identify the source of these overpotentials.

With the Nernst efficiency established, it was next desired to arrive at a system efficiency. The control volume is taken around the entire cell system. The useful work inside the control volume is divided into two parts. The first being the rate of thermodynamic energy being used to dissociate the CO₂. The second being the work required to electrochemically conduct the oxygen ions through the zirconia. The power passing into the control volume is also divided into two components. The first being the power delivered to the ceramic heaters, and the second being the power delivered to the electrolyte. The energy required to thermally dissociate the CO₂ is given by the equation:

$$\dot{Q}_{TH} = \sum_p N_i (\Delta h_f^\circ + h_T - h_{298})_i - \sum_r N_j (\Delta h_f^\circ + h_T - h_{298})_j$$

Here, Q_{TH} is the thermodynamic power input with the calculation showing the normal enthalpy of reaction equation with the enthalpy of formation and sensible enthalpies. The subscripts *i* and *j* represent the products and reactants respectively. The coefficient *N* represents the molar flow rate of each respective constituent. This value and the other power values give the following definition for the system efficiency:

$$\eta_{sys} = \frac{E_N I_{cell} + \dot{Q}_{TH}}{E_{cell} I_{cell} + E_{heat} I_{heat}}$$

In this equation, the subscript heat refers to observed values of the ceramic heater, and the subscript cell refers to observed values with the electrolyte, *E* being the potential (V) and *I* being the current (A). *Figure 14* displays the results of this analysis.

Summary

This paper has presented results from the first phase of a well-planned multiphase research program aimed at significantly reducing costs of future space missions; terrestrial applications are always

kept in mind. This proof of concept study has used full system hardware, realistic solid electrolytic cell material, realistic operating temperatures, full cell voltages, and full scale flow rates. These features distinguish our experiments from the usually understood test-tube demonstrations, where the conditions are substantially different from the real life counterpart. The only feature that is not duplicated here is the scale of oxygen production.

Important efficiencies are defined and measured. The basic electrolytic efficiency refers to the efficiency of using electrical input in producing oxygen, while the overall system efficiency refers to the enthalpy difference achieved between the product stream and the reactant stream divided by the overall energy input. The carbon dioxide flow rate, cell voltage, and cell temperature are all varied parametrically. A simple heat transfer theory explains the flow rate effects. The voltage effects are in good agreement with the manufacturer's specifications.

These thorough characterizations of the component performance parameters naturally lead us to the next step of scale-up and full system demonstration with active controls. Creative solutions to these engineering designs indicate that future space missions could realize substantial cost savings through the use of local (in-space) resources.

Acknowledgments

Research was supported by NASA Code R, through the University of Arizona Grant NAGW-1332. The authors are grateful to Murray Hirschbein and Gordon Johnston for funding and helpful comments.

References

- ¹Ash, R., Dowler, W., and Varsi, G., Feasibility of Rocket Propellant Production on Mars," *Acta Astronautica*, Vol. 5, 1978, pp. 705-724.
- ²Lawton, A.L., and Frisbee, R.H., "A New Look at Oxygen Production on Mars ISPP," Jet Propulsion Lab. Paper D-2661, Sept. 1986.
- ³Lawton, A.L., "Risk Factors in the Development of Zirconia Cell Technology for the Production of Oxygen from the Martian Atmosphere," Jet Propulsion Lab. Paper D-3546, Aug. 1986.
- ⁴Frisbee, R.H., "Mass and Power Estimates for Martian In-Situ Propellant Production Systems," Jet Propulsion Lab. Paper D-3648, Oct. 1986.
- ⁵Ramohalli, K., Lawton, E., and Ash, R., "Recent Concepts in Mission to Mars: Extraterrestrial Processes," *Journal of Propulsion and Power*, Vol. 5, No. 2, 1989, pp. 181-187.

⁶Richter, R., "Basic Investigation into the Production of Oxygen in a Solid Electrolyte," AIAA Paper 81-1175, June 1981.

⁷Suitor, J.W., Berdahl, C.M., Ferrall, J.F., Marner, W., Schroder, J.E., and Shichta, P.J., "Development of an Alternate Oxygen Production Source Using A Zirconia Solid Electrolyte Membrane," Jet Propulsion Lab. Paper D-4320, May 1987.

⁸Wark, K., *Thermodynamics*, 3rd ed., McGraw-Hill, New York, 1977, p. 840.

⁹Ash, R., Richter, R., Dowler, J.A., Hanson, and Uphoff, C.W., "Autonomous Oxygen for a Mars Return Vehicle," International Astronautical Federation Paper 82-210, 1982.

¹⁰Etsell, T.H., and Flengas, S.N., "Overpotential Behavior of Stabilized Zirconia Fuel Cells, *Journal of the Electrochemical Society*, Vol. 118, No. 12, 1971, pp. 1890-1900.